Effects of *D*-strain, *g*-strain, and dipolar interactions on EPR linewidths of the molecular magnets Fe$_8$ and Mn$_{12}$

Kyungwha Park,[1,*] M. A. Novotny,[1,†] N. S. Dalal,[2] S. Hill,[3,‡] and P. A. Rikvold[1,4]

[1]*School of Computational Science and Information Technology, Florida State University, Tallahassee, Florida 32306*
[2]*Department of Chemistry, Florida State University, Tallahassee, Florida 32306*
[3]*Department of Physics, Montana State University, Bozeman, Montana 59717*
[4]*Center for Materials Research and Technology and Department of Physics, Florida State University, Tallahassee, Florida 32306*

Electron paramagnetic resonance measurements on single crystals of the molecular magnets Fe$_8$ and Mn$_{12}$ reveal complex nonlinearities in the linewidths as functions of energy eigenstate, frequency, and temperature. Using a density-matrix equation with distributions of the uniaxial anisotropy parameter D, the Landé g factor, and dipolar interactions, we obtain linewidths in good agreement with experiments. Our study shows that the distribution in D is common to the examined molecular magnets Fe$_8$ and Mn$_{12}$ regardless of the qualities of the samples. This could provide the basis for a proposed tunneling mechanism due to lattice defects. The distribution in g is also quite significant for Mn$_{12}$.

PACS number(s): 75.45.+j, 75.50.Xx, 76.30.−v

I. INTRODUCTION

Molecular magnets such as Mn$_{12}$ (Ref. 1) and Fe$_8$ (Ref. 2) have recently drawn vigorous attention because of the macroscopic quantum tunneling (MQT) of their magnetizations at low temperatures[3,4] and their possible applications to quantum computing.[5] These materials consist of many identical clusters with the same magnetic properties and characteristic energies. Each cluster is made up of many different species of ions and atoms, with a total spin angular momentum in the ground state of $S=10$. The clusters have strong crystal-field anisotropy and thus a well-defined easy axis, and the magnetic interaction between different clusters is weak. Many competing models have been proposed to explain MQT in molecular magnets: higher-order transverse anisotropy,[6] thermally assisted quantum tunneling,[7,8] the Landau-Zener effect,[9–11] and dipolar interactions with dynamic hyperfine fields.[12] So far, the MQT in these materials has not been completely understood, and new experimental and theoretical approaches are needed.

In this paper, we present both previously unpublished experimental data and a theoretical model for the electron paramagnetic resonance (EPR) linewidths of single crystals of the molecular magnets Fe$_8$ and Mn$_{12}$ when the field is applied along the easy axis. To understand the measured linewidths, we use density-matrix equations, assuming that the uniaxial anisotropy parameter D and the Landé g factor are randomly distributed around their mean values (''D-strain'' and ''g-strain'' effects[13]) due to crystalline defects or impurities in samples. By adjusting the standard deviations of D and g, and the strength of the dipolar interactions, these equations are used to obtain theoretical linewidths in excellent quantitative agreement with our experimental data. Our theoretical study also shows that for the examined Fe$_8$ sample the distribution in D and the dipolar interactions are crucial to understand the linewidths, while for the Mn$_{12}$ sample the distributions in D and g are more important than the dipolar interactions. These results imply that the distribu-

tion in D seems to be generic in the molecular magnets Fe$_8$ and Mn$_{12}$, although the standard deviation of D itself varies between samples. This point assures that inherent defects or impurities in samples can be checked through the distribution in D by observing the linewidths of EPR spectra, and forms a basis of a recently proposed dislocation-induced tunneling mechanism.[14]

The experimental details are presented in Sec. II. Sec. III describes some typical EPR spectra and observed features, while Sec. IV presents our theoretical model. Section V discusses the theoretical results in comparison with the experimental data. Section VI describes our conclusions.

II. EXPERIMENTAL DETAILS

All the measurements were made on single crystals. Mn$_{12}$ was synthesized according to the procedure described by Lis.[1] Fe$_8$ was synthesized using Wieghart's method.[2] Single crystals of both materials were grown via slow evaporation. Typical crystal dimensions used were $1 \times 1 \times 0.5$ mm^3. EPR measurements were made for a magnetic field along or close to the easy axis using the multifrequency-resonator-based spectrometer described earlier.[15–18] The (transverse) excitation frequency was varied between 45 and 190 GHz. The temperature range was from 1.8 to 40 K, with a precision of 0.05 K. The linewidths were measured as functions of Zeeman field, EPR frequency, and temperature, for crystals of different quality, over a wide enough range to probe energy-level broadening due to lattice defects and inter-cluster dipolar interactions.

III. EXPERIMENTAL RESULTS

Figure 1 shows a typical EPR spectrum of Fe$_8$ for a field approximately along the easy axis at a resonance frequency of 133 GHz and at $T=10$ K.[16] Figure 2 shows a typical EPR spectrum of Mn$_{12}$ for a field along the easy axis at a resonance frequency of 169 GHz and $T=25$ K. The following interesting features are observed: the EPR linewidths are on
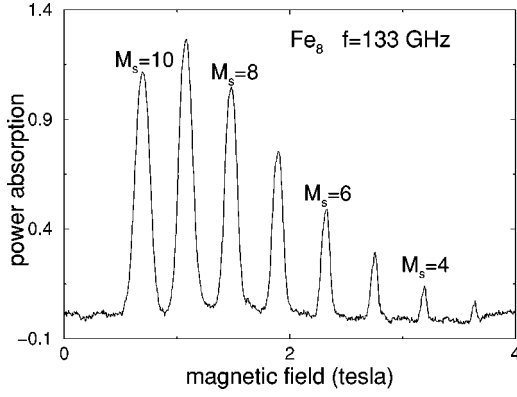
FIG. 1. Normalized power absorption (in arbitrary units) for Fe_8 as a function of magnetic field at $T=10$ K with the field almost along the easy axis ($\theta=9°$) (Ref. 16). Every other resonance peak is marked by the energy level from which the spin system is excited. For example, the leftmost peak is for the transition $M_s=10 \rightarrow 9$.

the order of several hundred to a thousand gauss for Fe_8 (one to a few thousand gauss for Mn_{12}) [Figs. 1, 2, and 3(a)–(d)]; the linewidths increase *nonlinearly* as a function of the absolute value of the energy eigenstate M_s [Figs. 1, 2, and 3(a)–(d)]; the minimum linewidths are observed for transitions involving the $M_s=0$ eigenstate, with a weak asymmetry in the widths about $M_s=0$ [Figs. 3(a) and (b)]; and resonances involving the same energy eigenstates become narrower upon increasing the measurement frequency or field [compare Fig. 3(a) with 3(c)].

IV. MODEL

For clarity, the model for Fe_8 is described separately from that for Mn_{12}.

A. Fe_8

To obtain the theoretical linewidths of the power absorption for Fe_8 clusters, we consider a single-spin system with
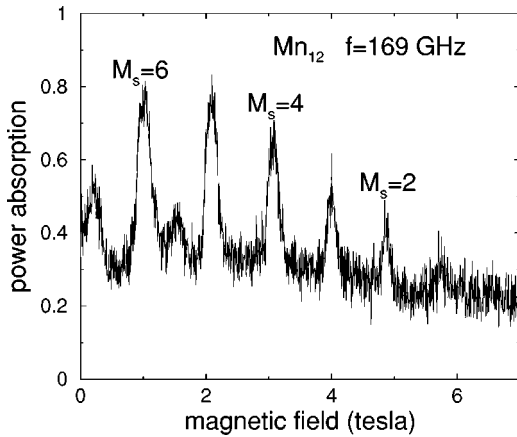

FIG. 2. Normalized power absorption (in arbitrary units) for Mn_{12} as a function of magnetic field at $T=25$ K with the field along the easy axis. Every other resonance peak is marked by the energy level from which the spin system is excited. The leftmost full resonance peak around 1 T is for the transition $M_s=6 \rightarrow 5$.
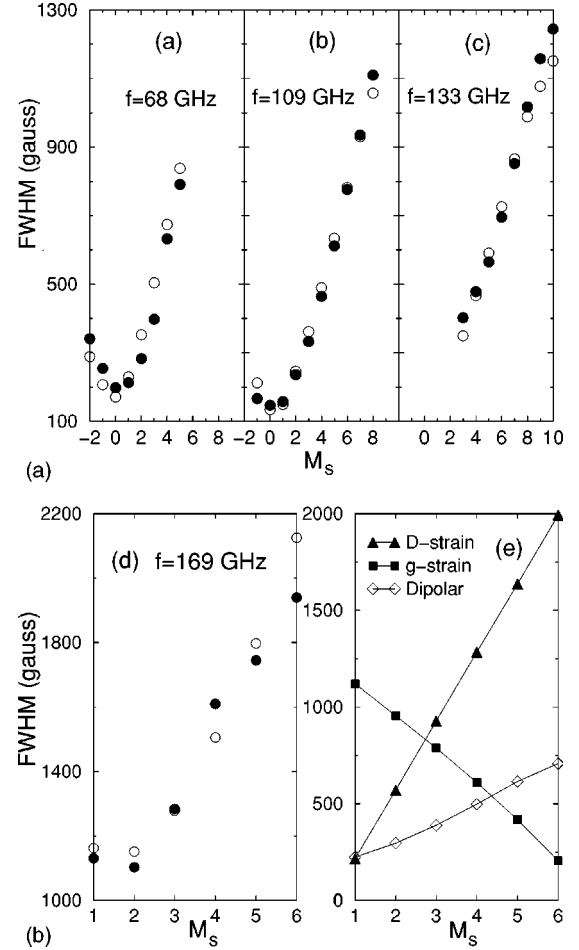

FIG. 3. Experimental (filled circles) and theoretical (open circles) full width at half maximum (FWHM) of the resonance lines vs M_s for (a), (b), (c) different frequencies at $T=10$ K for Fe_8, and (d) at $T=25$ K for Mn_{12}. (e) Line broadening due to D-strain, g-strain, and dipolar interactions vs M_s for the Mn_{12} sample in (d). The standard deviations of D and g, and the effective distance between dipoles for (e) are given below. Here $\vec{H} \parallel \hat{z}$. For Fe_8 (Mn_{12}), the fit is best when the standard deviation of D is $0.01D$ ($0.02D$ and the standard deviation of g is $0.008g$) and the effective distance between dipoles is 12 Å (14 Å).

$S=10$ in a weak oscillating transverse magnetic field. We choose the easy axis to be the z axis. Since the Fe_8 clusters have an approximate D_2 symmetry, the lowest-order ground-state single-spin Hamiltonian is[19]

$$\mathcal{H}_0 = -DS_z^2 - E(S_x^2 - S_y^2) - g\mu_B H_z S_z, \tag{1}$$

where $D=0.288k_B$ (k_B is Boltzmann constant) and the transverse crystal-field anisotropy parameter E is $0.043k_B$.[16] Here S_α is the αth component of the spin angular momentum operator, g is the Landé g factor which is close to 2, μ_B is the Bohr magneton, and H_z is the longitudinal static applied magnetic field. In zero field, ignoring the small transverse anisotropy terms, the eigenstates $(1/\sqrt{2})(|M_s\rangle \pm |-M_s\rangle)$ are degenerate for each M_s, and the lowest energy states are $(1/\sqrt{2})(|10\rangle \pm |-10\rangle)$. These degeneracies are lifted by applying the field H_z. When $H_z \approx D(m+m')/g\mu_B$, where m

and m' are eigenvalues of S_z in units of $\hbar$ ($m, m' = -10, \ldots, 10$), there exists a pair of quasidegenerate energy levels, m and m'. When H_z is large enough, the eigenvalue of S_z, M_s, is a good quantum number since the transverse terms are much smaller than the longitudinal terms. In such magnetic fields, the transverse terms, $E(S_x^2 - S_y^2)$, cause quantum tunneling between the two quasidegenerate energy levels. Next we introduce an interaction $V(t)$ between the spin system and an oscillating transverse magnetic field H_x with angular frequency $\omega \equiv 2\pi f$:

$$V(t) = \frac{V_0}{2}(e^{i\omega t} + e^{-i\omega t}), \quad V_0 \propto H_x S_x. \tag{2}$$

We treat $V(t)$ as a small perturbation to $\mathcal{H}_0$.

Besides the interaction $V(t)$, the spin system interacts with the environment, such as the thermal fluctuations of the clusters. Through this spin-phonon coupling, the spin system can relax to re-establish thermal equilibrium. Since the times of interest are much longer than the correlation time of the phonon heat bath, the heat bath is considered always to be in thermal equilibrium. Thus we can integrate out all degrees of freedom of the bath to obtain an equation of motion for the density matrix $\rho(t)$ of the spin system:[20]

$$\frac{d\rho(t)_{m',m}}{dt} = \frac{i}{\hbar}[\rho(t), \mathcal{H}_0 + V(t)]_{m',m} + \delta_{m',m}\sum_{n\neq m}\rho_{n,n}W_{mn}$$
$$- \gamma_{m',m}\rho_{m',m}, \tag{3}$$

$$\gamma_{m',m} = \frac{W_m + W_{m'}}{2}, \quad W_m = \sum_{k\neq m}W_{km}, \tag{4}$$

where the subscripts represent eigenstates of the longitudinal part of $\mathcal{H}_0$, $\rho(t)_{m'm} = \langle m'|\rho(t)|m\rangle$, and W_{km} is the transition rate from the mth to the kth eigenstate, which is determined by the spin-phonon coupling.[9]

We consider the case that the frequency ω of the oscillating field is fixed while H_z is varied to induce a resonance. With the selection rule $\Delta M_s = \pm 1$, the power absorbed between the M_s and the $M_s - 1$ level is

$$\frac{d\mathcal{E}}{dt} = \mathcal{E}_{M_s}[\dot{\rho}_{M_s,M_s}]_{\mathrm{rad}} + \mathcal{E}_{M_s-1}[\dot{\rho}_{M_s-1,M_s-1}]_{\mathrm{rad}}, \tag{5}$$

where $\mathcal{E}_{M_s}$ is the energy of the M_s level, and $[\dot{\rho}_{M_s,M_s}]_{\mathrm{rad}}$ is the change with time of the population in the level M_s caused by the first term in Eq. (3). We solve Eq. (3) for $[\dot{\rho}_{M_s,M_s}]_{\mathrm{rad}}$ up to first order in V_0 near resonance $[\omega \approx (\mathcal{E}_{M_s} - \mathcal{E}_{M_s-1})/\hbar]$. In this limit, among the many off-diagonal density-matrix elements, only $\rho(t)_{M_s-1,M_s}[=\rho(t)^*_{M_s,M_s-1}]$ contributes to $[\dot{\rho}_{M_s,M_s}]_{\mathrm{rad}}$. The matrix element $\rho(t)_{M_s-1,M_s}$ is obtained by solving Eq. (3). Consequently, only two neighboring energy levels are involved for each resonance peak. An increase of the population in one of the two energy levels results in a decrease of the population in the other. So the power absorption becomes[20]

$$\frac{d\mathcal{E}}{dt} = \frac{(\mathcal{E}_{M_s-1} - \mathcal{E}_{M_s})}{\hbar^2}\tilde{V}^2\Delta(H_z)(\rho_{M_s,M_s} - \rho_{M_s-1,M_s-1}),$$

$$\Delta(H_z) \equiv \frac{\hbar^2\gamma_{M_s-1,M_s}}{(g\mu_B)^2(H_z - H_{\mathrm{res}})^2 + (\hbar\gamma_{M_s-1,M_s})^2},$$

$$\tilde{V} \equiv |\langle M_s|V_0|M_s-1\rangle|, \quad H_{\mathrm{res}} \equiv \frac{\hbar\omega - D(2M_s-1)}{g\mu_B}, \tag{6}$$

where $\Delta(H_z)$ is a Lorentzian line-shape function, H_{res} is the resonant field, and $\hbar\gamma_{M_s-1,M_s}/g\mu_B$ gives a linewidth due to the finite lifetime of any excited state. As M_s decreases, the resonant field increases. The linewidth determined by $\gamma_{Ms-1,Ms}$ is on the order of several to several tens of gauss at temperatures below several tens of kelvin, and it increases as M_s decreases because of the corresponding shorter lifetimes. However, the experimentally observed linewidths *decrease* as M_s decreases until the $M_s = 1 \rightarrow 0$ and $M_s = 0 \rightarrow -1$ transitions (hereafter denoted $M_s = 1$ and $M_s = 0$, respectively), and are on the order of several hundred to a thousand gauss in the same temperature range [Figs. 1 and 3(a)–(c)].

To resolve these large discrepancies, we first assume that D and g are independent random variables with Gaussian distributions centered at $0.288k_B$ and 2.00, with standard deviations σ_D and σ_g, respectively. Such distributions can be caused by impurities or crystalline defects in the macroscopic sample, which result in different clusters seeing slightly different values of D and g. Then we calculate the average power absorption at a fixed frequency and $T = 10$ K by averaging Eq. (6) over the Gaussian distributions using MATHEMATICA,[21] to obtain the linewidth as a function of M_s. Our numerical calculations show that the distribution in D causes the linewidths to decrease linearly with decreasing absolute value of $2M_s - 1$, with a slight rounding close to the linewidth minimum ($M_s = 1,0$), where the D-strained linewidths approach the intrinsic lifetime broadening. On the other hand, the distribution in g makes the linewidths increase with decreasing M_s because the resonant field increases with decreasing M_s. These trends can be predicted from the expression for the resonant field H_{res} in Eq. (6) because the intrinsic linewidths are substantially smaller than the measured linewidths (with the exception of the lowest absolute M_s transitions). However, the density-matrix equation (3) is needed to understand the temperature dependence of the linewidths.

Next, we consider the effect of the intercluster dipolar interactions, in which each cluster experiences a net magnetic field comprised of the applied field and the dipolar fields from the surrounding clusters. At high temperatures ($k_B T \gg \hbar\omega$) these dipolar fields fluctuate randomly about zero, giving rise to a dipolar contribution to the EPR linewidths. At low temperatures, the ground state becomes preferentially populated, leading to nonzero dipolar fields which are the same at the site of each cluster. This leads to a line narrowing upon increasing H_{res} or the EPR frequency, or reducing the temperature. We use the multispin Hamiltonian that consists of $\mathcal{H}_0$ and $V(t)$ for each cluster, and magnetic

dipolar interactions between different clusters. We neglect the spin-phonon interaction because the spin-phonon relaxation time is very large compared to the spin-spin relaxation time. We truncate the original multispin Hamiltonian to leave only terms which commute with the z component of the total spin angular momentum $\Sigma_j S_{zj}$, where the sum runs over all clusters, because of the selection rule $\Delta \tilde{M}_s = \pm 1$ where $\tilde{M}_s$ is an eigenvalue of $\Sigma_j S_{zj}$. Then the dipolar interaction is modified to $\mathcal{H}^{dp} = \Sigma_{k>j} A_{jk}(\vec{S}_j \cdot \vec{S}_k - 3 S_{zj} S_{zk})$, where $A_{jk} \equiv [(g\mu_B)^2/2r_{jk}^3](3\zeta_{jk}^2 - 1)$. Here r_{jk} is the distance between clusters j and k, and ζ_{jk} is the direction cosine of r_{jk} relative to the z axis. Assuming that $\Sigma_j V_j(t) \ll \mathcal{H}^{dp} \ll \Sigma_j \mathcal{H}_{0j}$, we neglect $\Sigma_j V_j(t)$ in the energy of the multispin system and treat $\mathcal{H}^{dp}$ perturbatively. Following the formalism in the literature[22] for the $S = 10$ system, we calculate to first order in $\mathcal{H}^{dp}$ the root-mean-square deviation of the resonant field from the center value H_{res} in Eq. (6), assuming that the line is symmetric about the center value. We do not account for the exact geometry of the sample for this calculation. We use a lattice sum, assuming that dipoles are distributed on a simple cubic lattice, and the magnetic anisotropy axis is not particularly aligned along any of the edges of the lattice. The specific angles of the magnetic anisotropy axis with the lattice axes do not appreciably change the strength of the dipolar interactions. The dipolar interactions make the linewidths decrease as M_s decreases because the stronger resonant fields lead to a more polarized system.

In this study, we emphasize that the line broadening effect due to hyperfine fields does not appear to be a significant factor. Indeed, for Fe$_8$, there is no hyperfine splitting due to the metal ion, since the dominant Fe isotope, ^{56}Fe, has no nuclear spin.

The overall features of the linewidth, as a function of M_s, are determined by the competition among these three effects: D-strain, g-strain, and dipolar interactions. We have varied σ_D, σ_g, and the effective distance between the neighboring dipoles, d, within experimentally acceptable ranges in order to fit the experimental data.

B. Mn$_{12}$

Since the molecular magnet Mn$_{12}$ has tetragonal symmetry, the ground-state single-spin Hamiltonian is, to lowest order,

$$\mathcal{H}_0 = -DS_z^2 - CS_z^4 - g\mu_B H_z S_z \tag{7}$$

with $D = 0.55k_B$, $C = 1.17 \times 10^{-3} k_B$, and $g = 1.94$.[23] We perform the same analysis as in the previous subsection for the available Mn$_{12}$ data ($f = 169$ GHz, $T = 25$ K, the field along the easy axis); see Fig. 3(d). The differences are as follows: the resonant field is modified to

$$H_{res} \equiv \frac{\hbar\omega - D(2M_s - 1) + C(4M_s^3 - 6M_s^2 + 4M_s - 1)}{g\mu_B};$$

dipoles are assumed to be distributed on a bcc lattice, and the anisotropy axis is along the longer side of the sample.

For Mn$_{12}$, the hyperfine effect must be weak, because there is no resolved hyperfine splitting in the EPR spectra.

We attribute this absence of hyperfine splitting to exchange narrowing due to fast electron spin exchange over the metal-ion framework. Otherwise one would expect a linewidth of over 1000 G, since each ^{55}Mn nucleus ($I = \frac{5}{2}$) is expected to exhibit a hyperfine splitting of about 200 G.[19] Thus 12 almost equivalent ^{55}Mn nuclei, together with the acetate protons alone should lead to an overall width of over 1000 G. Notice that the measured smallest width [$M_s = 1$ in Fig. 3(d)] is about 1000 G, which increases to over 2000 G toward the transition $M_s = 10 \rightarrow 9$. The hyperfine effect would not be expected to change significantly with the electronic spin quantum number M_s. We thus consider the hyperfine effect as a lumped parameter representing the residual linewidth, independent of M_s.

V. RESULTS

For the Fe$_8$ sample examined, the calculated linewidths agree well with the experimental data at the measured frequencies ($f = 68$, 89, 109, 113, 133, and 141 GHz) at $T = 10$ K, using $\sigma_D \approx 0.01D$ and $d \approx 12$ Å. Within acceptable ranges of σ_D, σ_g, and d, no other combination of parameter values is able to produce the same quality of fit simultaneously to all of the frequencies studied, although other parameter values may produce good fits for a particular frequency. Figures 3(a)–(c) show the experimental and theoretical linewidths for Fe$_8$ at three frequencies. Our calculations show that the D-strain and the dipolar interactions are equally important for the linewidths of the sample, while the g-strain does not contribute significantly. It was previously speculated that M_s^2 dependence of the EPR linewidths for Fe$_8$ and Fe$_4$ was due to the D-strain only.[24] However, this cannot be explained by the D-strain alone, because the distribution in D only results in a *linear* M_s dependence of the linewidths. The possibility of the presence of dipolar fields was mentioned in a zero-field millimeter-wave experiment for Fe$_8$.[25] The weak asymmetry of the linewidths about $M_s = 1$ and $M_s = 0$, shown in Figs. 3(a) and (b), can be understood by combining the D-strain effect with the dipolar interactions. The D-strain produces linewidths symmetric about $M_s = 1$ and $M_s = 0$, while the dipolar interactions yield narrower linewidths with smaller M_s transitions, which are observed at higher resonant fields. For a given M_s transition, the linewidths decrease as the frequency increases because of the dipolar interactions. Compare Fig. 3(a) with Fig. 3(c). The distribution in D does not give frequency- or resonant-field dependent linewidths, but the dipolar interactions do. This is another reason that the distribution in D alone cannot explain the measured linewidths. We also considered distributions for other higher-order crystal-field anisotropy parameters (E or fourth-order coefficients) and found that they do not contribute substantially to the linewidths.

For the Mn$_{12}$ sample examined, the calculated linewidths [Fig. 3(d)] are in a good agreement with the experimental data for $\sigma_D \approx 0.02D$, $\sigma_g \approx 0.008g$, and $d \approx 14$ Å. Figure 3(e) shows separately the line broadening due to the D-strain, g-strain, and dipolar interactions with the chosen standard deviations and the effective distance between dipoles. For the Mn$_{12}$ sample, the distribution of D is wider than that for

the Fe_8 sample. The *D*-strain effect is still dominant, but a *g*-strain effect must be included as well to understand the linewidths for smaller M_s transitions. As shown in Fig. 3(e), the linewidths for $M_s = 2 \rightarrow 1$ and $M_s = 1 \rightarrow 0$ of over 1000 G cannot be explained by the *D*-strain and the dipolar interactions alone. It is essential to invoke the *g*-strain effect. The dipolar interactions do not play as significant a role as for the Fe_8 sample.

VI. CONCLUSIONS

We have presented our measured EPR spectra for the single-crystal molecular magnets Fe_8 and Mn_{12} as functions of energy eigenstate M_s and EPR frequency when the field is along the easy axis. We also have calculated theoretically the EPR linewidths to quantitatively compare with the experimental data, using density-matrix equations along with Gaussian distributions in *D* and *g* and the dipolar interactions. Our calculated linewidths agree well with the experimental data. Our analysis shows that for the examined Fe_8 sample the distribution in *D* and the dipolar interactions play key roles in explaining the linewidths, while for the Mn_{12} sample the distributions in *D* and *g* are more important than the dipolar interactions. From these, we draw the conclusion that the *D*-strain is universally important for the EPR linewidths in molecular magnets, although other effects, such as *g*-strain and dipolar interactions, can also contribute, depending on the material. These results imply that the assumption made in the tunneling model[14] may be correct. A distribution in *D* may also facilitate multiphoton transitions through virtual states which are necessary to implement a quantum algorithm for the molecular magnets Mn_{12} and Fe_8.[5] Additionally we speculate that the *D*-strain effect may contribute to the widths of resonant steps in magnetization hysteresis loops. A more detailed report,[26] including the temperature dependence of the linewidths at fixed frequency for both molecular magnets, will be published elsewhere.[27]

*Electronic address: park@csit.fsu.edu

†Present address: Department of Physics and Astronomy, Mississippi State University, Mississippi State, MS 39762.

‡Present address: Department of Physics, University of Florida, Gainesville, FL 32611.

[1] T. Lis, Acta Crystallogr., Sect. B: Struct. Crystallogr. Cryst. Chem. **B36**, 2042 (1980).

[2] K. Wieghart, K. Pohl, I. Jibril, and G. Huttner, Angew. Chem. Int. Ed. Engl. **23**, 77 (1984).

[3] J. Villain, R. Hartman-Boutron, R. Sessoli, and A. Rettori, Europhys. Lett. **27**, 159 (1994); *Quantum Tunneling of Magnetization–QTM '94*, Vol. 301 of *NATO Advanced Study Institute, Series E: Applied Sciences*, edited by L. Gunther and B. Barbara (Kluwer, Dordrecht, 1995).

[4] E.M. Chudnovsky and J. Tejada, *Macroscopic Quantum Tunneling of the Magnetic Moment*, Cambridge Studies in Magnetism Vol. 4 (Cambridge University Press, Cambridge, 1998), and references therein.

[5] M.N. Leuenberger and D. Loss, Nature (London) **410**, 789 (2001).

[6] F. Hartmann-Boutron, P. Politi, and J. Villain, Int. J. Mod. Phys. B **10**, 2577 (1996); A. Fort, A. Rettori, J. Villain, D. Gatteschi, and R. Sessoli, Phys. Rev. Lett. **80**, 612 (1998).

[7] J. Friedman, M.P. Sarachik, J. Tejada, and R. Ziolo, Phys. Rev. Lett. **76**, 3830 (1996); D.A. Garanin and E.M. Chudnovsky, Phys. Rev. B **56**, 11 102 (1997); F. Luis, D. J. Bartolomé, and F. Fernández, *ibid.* **57**, 505 (1998).

[8] M.N. Leuenberger and D. Loss, Phys. Rev. B **61**, 1286 (2000).

[9] M.N. Leuenberger and D. Loss, Phys. Rev. B **61**, 12 200 (2000).

[10] H. De Raedt, S. Miyashita, K. Saito, D. Garciá-Pablos, and N. García, Phys. Rev. B **56**, 11 761 (1997).

[11] V.V. Dobrovitsky and A.K. Zvezdin, Europhys. Lett. **38**, 377 (1997).

[12] N.V. Prokof'ev and P.C.E. Stamp, Phys. Rev. Lett. **80**, 5794 (1998); W. Wernsdorfer, T. Ohm, C. Sangregorio, R. Sessoli, D. Mailly, and C. Paulsen, *ibid.* **82**, 3903 (1999).

[13] J.R. Pilbrow, *Transition Ion Electron Paramagnetic Resonance* (Clarendon, Oxford, 1990).

[14] E.M. Chudnovsky and D.A. Garanin, Phys. Rev. Lett **87**, 187203 (2001); cond-mat/0105518 (unpublished).

[15] S. Hill, J.A.A.J. Perenboom, N.S. Dalal, T. Hathaway, T. Stalcup, and J.S. Brooks, Phys. Rev. Lett. **80**, 2453 (1998).

[16] S. Maccagnano, R. Achey, E. Negusse, A. Lussier, M.M. Mola, S. Hill, and N.S. Dalal, Polyhedron **20**, 1441 (2001).

[17] J.A.A.J. Perenboom, J.S. Brooks, S. Hill, T. Hathaway, and N.S. Dalal, Phys. Rev. B **58**, 330 (1998); E. del Barco, J.M. Hernandez, J. Tejada, N. Biskup, R. Achey, I. Rutel, N. Dalal, and J. Brooks, *ibid.* **62**, 3018 (2000).

[18] S. Hill, N.S. Dalal, and J.S. Brooks, Appl. Magn. Reson. **16**, 237 (1999).

[19] A. Abragam and B. Bleaney, *Electron Paramagnetic Resonance of Transition Ions* (Clarendon, Oxford, 1970).

[20] K. Blum, *Density Matrix Theory and Applications*, 2nd edition (Plenum, New York, 1996).

[21] S. Wolfram, *The Mathematica Book*, 3rd ed. (Wolfram Media/Cambridge University Press, New York, 1996).

[22] J.H. Van Vleck, Phys. Rev. **74**, 1168 (1948); M. McMillan and W. Opechowski, Can. J. Phys. **38**, 1168 (1960).

[23] A.L. Barra, D. Gatteschi, and R. Sessoli, Phys. Rev. B **56**, 8192 (1997).

[24] A.L. Barra, D. Gatteschi, and R. Sessoli, Chem.-Eur. J. **6**, 1608 (2000); A. Bouwen, A. Caneschi, D. Gatteschi, E. Goovaerts, D. Schoemaker, L. Sorace, and M. Stefan, cond-mat/0101255 (unpublished).

[25] A. Mukhin, B. Gorshunov, M. Dressel, C. Sangregorio, and D. Gatteschi, Phys. Rev. B **63**, 214411 (2001).

[26] Extension of this model to a full line-shape analysis indicates that it might be possible to distinguish between the distributions due to various types of physical mechanisms, including edge dislocations.

[27] K. Park, M.A. Novotny, N.S. Dalal, S. Hill, and P.A. Rikvold (unpublished).